# Enhancement of luminous flux and color quality of white light-emitting diodes by using green (Y,Gd)BO$_3$:Tb$^{3+}$ phosphor

**My Hanh Nguyen Thi[1], Phung Ton That[2], Nguyen Doan Quoc Anh[3]**
[1]Faculty of Mechanical Engineering, Industrial University of Ho Chi Minh City, Vietnam
[2]Faculty of Electronics Technology, Industrial University of Ho Chi Minh City, Vietnam
[3]Power System Optimization Research Group, Faculty of Electrical and Electronics Engineering, Ton Duc Thang University, Ho Chi Minh City, Vietnam

| Article Info | ABSTRACT |
|---|---|
| | In the study, we analyzed and clarified the effect of green (Y,Gd)BO$_3$:Tb$^{3+}$ phosphor on chromatic homogeneity and optical performance of multi-chip white light emitting diodes (MCW-LEDs). Thereby there is a solution to get the best luminous efficiency. In addition, (Y,Gd)BO$_3$:Tb$^{3+}$ is known as one of the factors that has a significant impact on lighting performance, so it needs to add the (Y,Gd)BO$_3$:Tb$^{3+}$ phosphor in the structure of LEDs to combine with the yellow phosphor YAG:Ce$^{3+}$ to receive the best results. Therefore, the concentration and size of (Y,Gd)BO$_3$:Tb$^{3+}$ should be choose carefully so that the presentation of MCW-LEDs would be more incredible. The results show that when the concentration of green-emitting (Y,Gd)BO$_3$:Tb$^{3+}$ phosphor tends to increase, it also helps the color homogeneity and the lumen efficiency of MCW-LEDs with the average correlated color temperature (CCT) of 5600 K-8500 K become better.<br><br>*This is an open access article under the CC BY-SA license.*<br><br> |

***Corresponding Author:***

Nguyen Doan Quoc Anh
Power System Optimization Research Group, Faculty of Electrical and Electronics Engineering
Ton Duc Thang University
No. 19 Nguyen Huu Tho Street, Tan Phong Ward, District 7, Ho Chi Minh City, Vietnam
Email: nguyendoanquocanh@tdtu.edu.vn

## 1. INTRODUCTION

In recent years, researchers have been always aiming to obtain the improvement in the light efficiency of white LEDs. In addition, they also have put a lot of effort into achieving better optical output and color uniformity for white light emitting diodes (LEDs) [1-3]. Finally, Anh and his colleague recognized a truth that the performance of multi-chip white LED (MCW-LED) lights can be promoted through the mixture of YAG:Ce$^{3+}$ phosphor with SiO$_2$ particles [4]. Moreover, the yellow YAG:Ce$^{3+}$ phosphor should be blended with the silicone glue so that it could create a mixture that emits yellow light and absorbs blue light emitted from blue chips, and then generates white light. Before white lights are generated, the lights need to go through two processes: first, disintegrating in phosphorus compounds, and second, transmitting through phosphorus particles [5-8]. During this process, the yellow YAG:Ce$^{3+}$ phosphor particles will absorb the blue-light energy and weaken it. However, after every scattering the converted yellow light bcomes more vehement. In addition, the light intensity distribution also affects the color of the LED light. Specifically, the emitted light will become more bluish as it reaches the surface of LED, while it tends to be more yellowish when it is almost parallel to the surface of the LED. Thus, if the distribution of the light intensity changes, it can result in a yellow circle surrounding the white light, which is also known as yellow ring phenomenon [9-12]. When the white light

quality and lumen output receive the optimized methods for phosphorus or optical structure of white LEDs, there will be a positive difference. Won, together with his partner, proved the strong influence of phosphor geometry on the luminous intensity of white light emitting diode (WLED) devices yielding better color quality scale (CQS). In this project, they combined the LED chips with green $(Ba,Sr)_2SiO_4:Eu^{2+}$ and red $CaAlSiN_3:Eu^{2+}$ phosphors with various phosphor designs to achieve optimal efficiency [13-15]. However, when the Green-Amber-Red multi-package LED is proposed, its priority is to obtain the best lumen output and CRI [16-20]. The multi-chromatic phosphor is used in order to serve a purpose in attaining the better quality for the CRI of the LED lamp. The problem that scientists have always been concerned about is how to improve CRI and optical output, but they ignore the enhancement in the uniformity of correlated color temperature (CCT). Moreover, the WLED packages these articles concentrated on is the single-chip one. In other words, their results did not really work with high CCT multi-chip white LEDs [21-23].

In this paper, the participation of green $(Y,Gd)BO_3:Tb^{3+}$ phosphor helps the chromatic homogeneity and the luminous performance positively transform in the phosphorus compound utilized in MCW-LEDs during the light scattering process. Depending on the density of $(Y,Gd)BO_3:Tb^{3+}$ particles, it will propose the development trend of the lighting quality as well as the color homogeneity. The research contains 3 stages: 1) building the model of MCW-LEDs; 2) blending $(Y,Gd)BO_3:Tb^{3+}$ with the phosphor compound in the simulated MCW-LEDs; 3) carrying out the investigation on how $(Y,Gd)BO_3:Tb^{3+}$ concentration affect the optical performance, such as the emission spectra and the scattering. To sum up, if $(Y,Gd)BO_3:Tb^{3+}$ and $YAG:Ce^{3+}$ phosphors are used in LED structures, it will contribute to improving the uniformity of light color and the luminous flux.

## 2. PREPARATION AND SIMULATION

### 2.1. Preparation of green $(Y,Gd)BO_3:Tb^{3+}$ phosphor

$(Y,Gd)BO_3:Tb^{3+}$ is a potential phosphor material for LED packages due to their high luminous efficiency. Before starting the preparation process, it is essential to understand the nature of $(Y,Gd)BO_3:Tb^{3+}$. It comprises four grassroots: 51.9 g of $Y_2O_3$ (accounting for 23% of the compound), 83.4 gram of $Gd_2O_3$ (having the same percentage with $Y_2O_3$), 15 grams of $Tb_4O_7$ (very small amount) and 85.9 gram of $H_3BO_3$ (major mole). The process of fabricating $(Y,Gd)BO_3:Tb^{3+}$ is demonstrated as follows. Initially, dry blending above ingredients. Next, firing the mixture in capped quartz tubes with air flows and at 400-500$^0$C for 2 hours. After that, putting slurry powder in boiling 10% HCI for 30 minutes. Then, decanting it with boiling water until neutral. Finally, drying it at 110$^0$C. The process of creating $(Y,Gd)BO_3:Tb^{3+}$ is seen as successful when the mixture can requires the following optical properties. During the emission, the compound has green color. In addition, its emission peak is 544 mm, and -3.40 eV, +4.88 eV and +8.40 eV are the index of excitation efficiency by UV.

### 2.2. MC-WLED simulation

LightTools 8.1.0 program and the Monte Carlo method are applied to construct the MC-WLEDs simulation with the addition of green phosphor $(Y,Gd)BO_3:Tb^{3+}$. Moreover, it is crucial to observe and evaluate the influences of $(Y,Gd)BO_3:Tb^{3+}$ concentrations on the optical performance of W-LED packages, see Figure 1 (a) and Figure 1 (b). Additionally, the WLED used in the study has average CCT of 5600 K and 8500 K. The reflector, one of the elements comprising WLED lamp, has parameters of 8 mm in bottom length, 2.07 mm in height, and 9.85 mm in top surface length. Each LED chip embedded to the reflector's cavity owns 1.14 mm$^2$ square base area, a height of 0.15 mm, the radiant power of 1.16 W, and a wavelength that peaks at 453 nm. The 0.08 mm thick phosphor layers are placed over the nine LED chips. Figure 1 (c) shows a clear description of a MCW-LED package with remote phosphor structure of two phosphor layers: yellow $YAG:Ce^{3+}$ and green $(Y,Gd)BO_3:Tb^{3+}$ layers. Moreover, it is important to note that the green phosphor $(Y,Gd)BO_3:Tb^{3+}$ is above the yellow $YAG:Ce^{3+}$ layer.
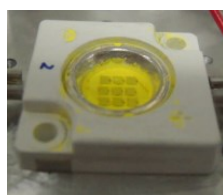
Lead frame: 4.7 mm Jentech Size-S
LED chip: V45H
Die attach: Sumitomo 1295SA

Gold Wire: 1.0 mil
Phosphor: ITC NYAG4_EL
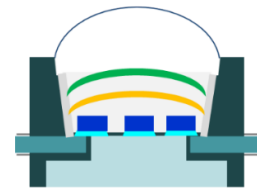
(a) (b) (c)

Figure 1. Illustration of phosphor-converted MCW-LEDs as doping $(Y,Gd)BO_3:Tb^{3+}$: (a) The actual MCW-LEDs, (b) its parameters, and (c) dual-remote phosphor configuration

By applying the Mie-theory, the scattering of phosphor particles can be analyzed easily. In this study, the actual parameter average diameter for all phosphorus particles was 14.5 mm. Figure 2 describes the emission spectra of WLEDs with a dual-remote phosphor compound doping 10% $(Y,Gd)BO_3:Tb^{3+}$. It can be seen obviously from this chart that the yielded luminescence of MCW-LEDs becomes better after $(Y,Gd)BO_3:Tb^{3+}$ particles are added into phosphor compound.
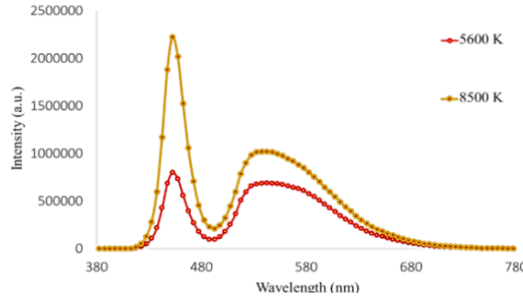


Figure 2. Emission spectra of MCW-LEDs

## 3. COMPUTATION AND DISCUSSION

The Mie-scattering theory [24-26] plays an inprotant role in carrying out the computation of scattering coefficient $\mu_{sca}$ to verify optical properties of phosphor compounding. The connection among the scattering coefficient (SC), the wavelength, and the size of $(Y,Gd)BO_3:Tb^{3+}$ particles is described by the following equations:

Here, $f(D)$ is the size distribution function, $c$ is the phosphor concentration ($g/cm^3$), $C_{sca,D}$ is the scattering cross-section of the phosphor with a particle diameter of D. $\bar{C}_{sca}(\lambda)$ indicates the scattering cross-section and $\bar{m}$ shows the particle mass of the phosphor integrated over f(D). $P_{sca}(\lambda)$ and $I_{inc}(\lambda)$ are the scattered power by phosphor particles and the irradiance intensity, respectively.

$$\mu_{sca}(\lambda) = \frac{c}{\bar{m}}\bar{C}_{sca}(\lambda) \tag{1}$$

$$\bar{C}_{sca}(\lambda) = \frac{\int^{\int} C_{sca,D}(\lambda)f(D)dD}{\int^{\int} f(D)dD} \tag{2}$$

$$\bar{m} = \frac{\int^{\int} m_i(D)f(D)dD}{\int^{\int} f(D)dD} \tag{3}$$

$$C_{sca}(\lambda) = \frac{P_{sca}(\lambda)}{I_{inc}(\lambda)} \tag{4}$$

According to Figure 3, we calculate the scattering coefficient through the scattering process of $(Y,Gd)BO_3:Tb^{3+}$ phosphor. The concentrations and different triggers of $(Y,Gd)BO_3:Tb^{3+}$ will be a catalyst that causes SC of the phosphor compound to fluctuate significantly. When the concentration of $(Y,Gd)BO_3:Tb^{3+}$ increases, SC also become higher at any particle size of $(Y,Gd)BO_3:Tb^{3+}$ phosphor. With a size of approximately 1 μm, SC reaches the highest value as well as makes the color uniformity develop better. Hence, the $(Y,Gd)BO_3:Tb^{3+}$ size of approximately 1 μm should be chosen if the target is CQS. Otherwise, it is around 7 μm, the SC of the phosphor layer tends to be much more steady without concerning the increase in $(Y,Gd)BO_3:Tb^{3+}$ concentration, which gives the color quality (CQS) of the LEDs so many benefits. As a result, if the target is CQS, the lighter size of 7 μm can be selected. Obviously, the SC value is dependent on not only the concentration but also the size of $(Y,Gd)BO_3:Tb^{3+}$, which is the reason why $(Y,Gd)BO_3:Tb^{3+}$ is recommended for the enhancement of the lumen efficacy and color quality of WLEDs.

In this article, the LED product specification must be strictly adhered. Hence, the enhancement of MCW-LED should be bound with the average CCTs. Accordingly, when the concentration of the $(Y,Gd)BO_3:Tb^{3+}$ phosphor increases, a strong reduction in yellow phosphor $YAG:Ce^{3+}$ concentration is required for stabilizing the average CCTs. The CCT peak-valley deviation tends to decrease sharply when the concentration of $(Y,Gd)BO_3:Tb^{3+}$ increases, as can be seen in Figure 4. In other words, the spatial color distribution of MCW-LEDs with $(Y,Gd)BO_3:Tb^{3+}$ is much flatter compared to the absence of $(Y,Gd)BO_3:Tb^{3+}$.

To accomplish the best improvement for WLED packages, it is important to ensure that performance properties and optimization issues are in balance. In other words, we need to focus on advancing both of them, not just focus on one element as this will make the optical system become weak in the other aspect, or in another manner, CQS and the luminescence efficacy of a white LED lamp cannot contemporaneously achieve the best results. Therefore, we need to obtain good CRI, and at the same time, a broad source spectrum and efficiency must be maximized at monochromatic radiation with a wavelength of 555 nm. Considering this issue, the paper makes the indexes of CQS, lumen output, and the P-V deviation of CCT three competitors. In Figure 5 and Figure 6, the lumen output and the color quality scale are described following the concentration of $(Y,Gd)BO_3:Tb^{3+}$. As can be seen, the increase in $(Y,Gd)BO_3:Tb^{3+}$ concentration will support the enhancement of the luminous flux, but will degrade the CQS. However, if there is a small reduction in the concentration of $(Y,Gd)BO_3:Tb^{3+}$, it will help to increase both the CCT homogeneity and the luminescence efficacy.



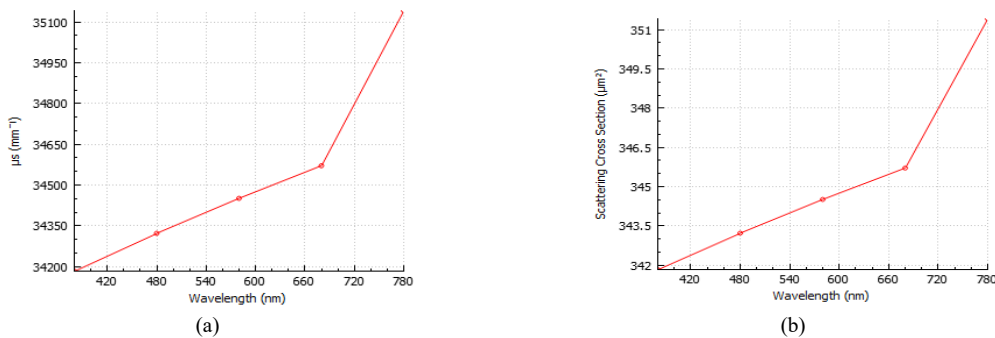(a)                                                      (b)

Figure 3. Phosphor compounding; (a) the computed values of scattering coefficients, and (b) scattering cross-section
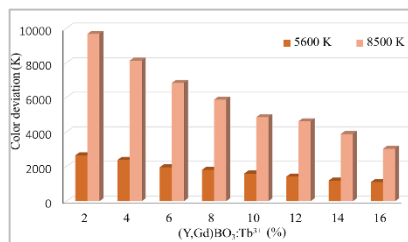


Figure 4. The CCT peak-valley deviation as a function of the concentration of $(Y,Gd)BO_3:Tb^{3+}$
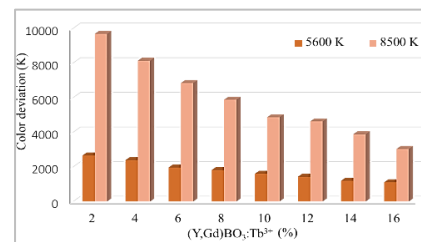
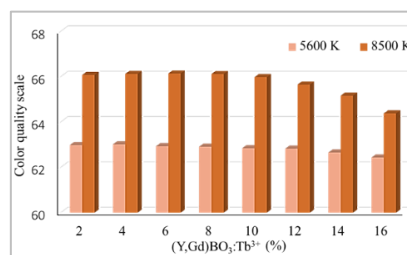Figure 5. Luminous flux as a function of the concentration of $(Y,Gd)BO_3:Tb^{3+}$



Figure 6. Color quality scale as a function of the concentration of $(Y,Gd)BO_3:Tb^{3+}$

## 4.    CONCLUSION

In conclusion, the potency of using green $(Y,Gd)BO_3:Tb^{3+}$ phosphor in the process of acquiring better performance for CCT uniformity and luminous intensity of white LED devices is demonstrated through findings in the article. Firstly, according to Mie scattering theory, the color uniformity is very diverse, regardless of the average CCT value, because of the light-scattering compensation to the WLEDs. Besides that, with the support from Monte Carlo simulation, the difference in lumen values is presented and

discussed by concentration-dependent $(Y,Gd)BO_3:Tb^{3+}$. Indeed, the lumen output increases together with the change of $(Y,Gd)BO_3:Tb^{3+}$ concentration. Meanwhile, that increase leads to a decrease in CQS. However, if we reduce a small amount of $(Y,Gd)BO_3:Tb^{3+}$ concentration, the LED structure can attain better CQS and luminous flux. In short, $(Y,Gd)BO_3:Tb^{3+}$ phosphor can be a right answer for the inquiry into the development of optical properties of phosphorus layers and MCW-LED fabrication.

## REFERENCES

[1] V. Fuertes *et al.*, "Enhanced luminescence in rare-earth-free fast-sintering glass-ceramic," *Optica*, vol. 6, no. 5, pp. 668-679, 2019.

[2] X. Huang et al., "High-brightness and high-color purity red-emitting Ca3Lu, AlO.3, BO3.4:Eu3+ phosphors with internal quantum efficiency close to unity for near-ultraviolet-based white-light-emitting diodes," *Opt. Lett*, vol. 43, no. 6, pp. 1307-1310, 2018.

[3] W. Gao et al., "Color temperature tunable phosphor-coated white LEDs with excellent photometric and colorimetric performances," *Opt. Express,* vol. 57, no. 31, pp. 9322-9327, 2018.

[4] H. L. Ke et al., "Lumen degradation analysis of LED lamps based on the subsystem isolation method," *Appl. Opt,* vol. 57, no. 4, pp. 849-854, 2018.

[5] S. Beldi et al., "High Q-factor near infrared and visible Al2O3-based parallel-plate capacitor kinetic inductance detectors," *Opt. Express,* vol. 27, no. 9, pp. 13319-13328, 2019.

[6] H. Liu et al., "Design of a six-gas NDIR gas sensor using an integrated optical gas chamber," *Opt. Express,* vol. 28, no. 8, pp. 11451-11462, 2020.

[7] D. Lu et al., "Synthesis and photoluminescence characteristics of the LiGd3, MoO4.5:Eu3+ red phosphor with high color purity and brightness," *Opt. Mater. Express,* vol. 8, no. 2, pp. 259-269, 2018.

[8] L. Wu et al., "Hybrid warm-white organic light-emitting device based on tandem structure," *Opt. Express,* vol. 26, no. 26, pp. A996-A1006, 2018.

[9] S. Elmalem et al., "Learned phase coded aperture for the benefit of depth of field extension," *Opt. Express,* vol. 26, no. 12, pp. 15316-15331, 2018.

[10] J. H. Kim et al., "Synthesis of Mn-doped CuGaS2 quantum dots and their application as single downconverters for high-color rendering solid-state lighting devices," *Opt. Mater. Express,* vol. 8, no. 2, pp. 221-230, 2018.

[11] C. Tian et al., "$Mn^{4+}$ activated $Al_2O_3$ red-emitting ceramic phosphor with excellent thermal conductivity," *Opt. Express,* vol. 27, no. 22, pp. 32666-32678, 2019.

[12] X. D. Leng et al., "Feasibility of co-registered ultrasound and acoustic-resolution photoacoustic imaging of human colorectal cancer," *Biomed. Opt. Express,* vol. 9, no. 11, pp. 5159-5172, 2018.

[13] H. S. E. Ghoroury et al., "Color temperature tunable white light based on monolithic color-tunable light emitting diodes," *Opt. Express,* vol. 28, no. 2, pp. 1206-1215, 2020.

[14] J. Cheng et al., "Photoluminescence properties of Ca4La6, SiO4.4, PO4.2O2-based phosphors for wLEDs," *Chin. Opt. Lett*, vol. 17, no. 5, pp. 051602-, 2019.

[15] Y. Yang et al., "Low complexity OFDM VLC system enabled by spatial summing modulation," *Opt. Express,* vol. 27, no. 21, pp. 30788-30795, 2019.

[16] L. He et al., "Performance enhancement of AlGaN-based 365 nm ultraviolet light-emitting diodes with a band-engineering last quantum barrier," *Opt. Lett*, vol. 43, pp. 515-518, 2018.

[17] Y. Wang et al., "Controlling optical temperature behaviors of $Er^{3+}$ doped $Sr_2CaWO_6$ through doping and changing excitation powers," *Opt. Mater. Express,* vol. 8, no. 7, pp. 1926-1939, 2018.

[18] J. Ji et al., "Theoretical analysis of a white-light LED array based on a GaN nanorod structure," *Appl. Opt,* vol. 59, no. 8, pp. 2345-2351, 2020.

[19] W. Wang et al., "On the development of an effective image acquisition system for diamond quality grading," *Appl. Opt,* vol. 57, no. 33, pp. 9887-9897, 2018.

[20] Y. F. Huang et al., "Red/green/blue LD mixed white-light communication at 6500K with divergent diffuser optimization," *Opt. Express,* vol. 26, no. 18, pp. 23397-23410, 2018.

[21] O. Kunieda et al., "High-quality full-parallax full-color three-dimensional image reconstructed by stacking large-scale computer-generated volume holograms," *Appl. Opt*, vol. 58, no. 34, pp. G104-G111, 2019.

[22] A. Krohn et al., "LCD-Based Optical Filtering Suitable for Non-Imaging Channel Decorrelation in VLC Applications," *J. Lightwave Technol*, vol. 37, no. 23, pp. 5892-5898, 2019.

[23] B. Qiu et al., "Synthesis and enhanced luminescent properties of SiO2@LaPO4:Ce3+/Tb3+ microspheres," *Opt. Mater. Express,* vol. 8, no. 1, pp. 59-65, 2018.

[24] Y. Zhang et al., "Modeling and optimizing the chromatic holographic waveguide display system," *Appl. Opt*, vol. 58, no. 34, pp. G84-G90, 2019.

[25] Q. T. Vinh et al., "Preliminary measure for the characterization of the usefulness of light sources," *Opt. Express,* vol. 26, no. 11, pp. 14538-14551, 2018.

[26] H. P. Huang et al., "White appearance of a tablet display under different ambient lighting conditions," *Opt. Express,* vol. 26, no. 4, pp. 5018-5030, 2018.